

# Thermoelectric Properties of the Semiconducting Chevrel Phase $\text{Mo}_2\text{Re}_4\text{Se}_8$

T. Caillat and J. -P. Fleurial

Jet Propulsion Laboratory  
California Institute of Technology  
4800 Oak Grove Drive  
Pasadena, CA 91109

## Abstract

We have prepared and measured the electrical resistivity, Seebeck coefficient, and thermal conductivity of the Chevrel material  $\text{Mo}_2\text{Re}_4\text{Se}_8$  in the 300-1000K temperature range. The results show that  $\text{Mo}_2\text{Re}_4\text{Se}_8$  is a semiconductor with a relatively low thermal conductivity. The semiconducting nature of this compound is consistent with theoretical predictions based on the number of valence electrons per  $[\text{Mo}_6]$  cluster. The crystal structure of Chevrel phases contains several voids of different sizes and shapes which can be filled by a variety of atomic elements. The filling of these interstices may be used as a means to achieve low thermal conductivity values by increasing the phonon scattering. This represents an attractive possibility considering that low thermal conductivity is one of the requirements for a good thermoelectric material. Various approaches to determine the potential of Chevrel phases for thermoelectric applications are presented and discussed.

**Keywords:** A. chalcogenides, A. semiconductors D. transport properties.

## Introduction

Ternary chalcogenides of formula  $\text{M}_x\text{Mo}_6\text{X}_8$  ( $\text{M} = \text{Cu}, \text{Ag}, \text{Ni}, \text{Fe}, \text{rare earth, etc.}$ ) and  $\text{X} = \text{S}, \text{Se}, \text{or Te}$  have been known since the 1970's. They have attracted considerable interest because of their superconducting properties with large critical magnetic fields [1]. They were first synthesized by Chevrel et al. in 1971 [2] and therefore are often referred to as Chevrel compounds. The ternary phases have structures closely related to those of binary molybdenum chalcogenides  $\text{Mo}_6\text{X}_8$  ( $\text{X} = \text{S}, \text{Se}, \text{Te}$ ). The  $\text{Mo}_6\text{X}_8$  unit is illustrated in Figure 1 and consists of an  $[\text{Mo}_6]$  octahedron "cluster" surrounded by eight chalcogens arranged in a distorted cube. The rhombohedral Chevrel phase consists of a stacking of  $\text{Mo}_6\text{X}_8$  units and contains channels where additional metal atoms can be inserted, forming  $\text{MMo}_6\text{X}_8$  ternary compounds. One additional feature of the Chevrel phases is the great flexibility of the crystal structure which allows all the constituents of the ternary phases to be substituted by a variety of elements with a wide range of mass, size, electronegativity and composition.

Many of the physical properties of the Chevrel phases appear to be linked to the number of electrons per Mo atom in the cluster. This quantity, often referred to as “cluster-valence-electron” (cluster-VEC) is calculated by adding the valence electrons of the atoms M to the valence electrons of Mo, by subtracting the number of electrons required to “fill” the octets of the chalcogen atoms and dividing the result by the number of Mo atoms [5]. Chevrel phases are formed for cluster VEC numbers between 3.3 and 4. [5]. In addition, band structure calculations results predicted an energy gap in the electronic structure for 4 valence electrons per Mo atom in the cluster [6]. The cluster VEC of Chevrel phases varies between 3.3 ( $\text{Mo}_6\text{Se}_8$ ) to a maximum value of 4 for  $\text{M}_x\text{Mo}_6\text{Se}_8$  compounds. In particular, the “magic” number of 4 is met in the compound  $\text{Cu}_4\text{Mo}_6\text{Se}_8$  although the semiconducting nature of this compound was not confirmed experimentally. Values of 4 are also attained in mixed-metal cluster compounds such as  $\text{Mo}_2\text{Re}_4\text{Se}_8$  and  $\text{Mo}_4\text{Ru}_2\text{Se}_8$  [3,4] and these compounds were found to be semiconductors, supporting the idea of an energy gap in the band structure of the Chevrel phases with a “magic” cluster VEC number of 4.

As we mentioned above, these compounds have been mainly investigated for their superconducting properties. A recent interest in studying and developing new classes of thermoelectric materials has been motivated by the identification of several new promising materials, including skutterudites [7,8]. Studies on skutterudites initially focused on binary compounds but it became soon clear that thermoelectric figures of merit (ZT) greater than those obtained for state-of-the-art thermoelectric materials would not be achieved if the lattice thermal conductivity could not be significantly reduced. One of the features of the skutterudite compounds is the presence of holes in the structure. These holes can be filled by various atoms which have been shown to produce an important phonon scattering, resulting in a significant reduction in lattice thermal conductivity and superior thermoelectric properties [7-10]. As we mentioned before, the Chevrel phases also contain interstices which can be filled with a variety of atoms which may effectively scatter phonons like in skutterudites, resulting in low thermal conductivity which is one of the requirements for a good thermoelectric. We have started to synthesize some of the presumably semiconducting Chevrel phases to assess their potential for thermoelectric applications. To the best of our knowledge, no data exists on the thermoelectric properties of Chevrel phases. We have chosen to start with the compound  $\text{Mo}_2\text{Re}_4\text{Se}_8$  and report here on its thermoelectric properties.

## Experimental details

Single phase, polycrystalline samples of  $\text{Mo}_2\text{Re}_4\text{Se}_8$  were prepared by mixing and reacting stoichiometric amounts of molybdenum (99.999%), rhenium (99.997%), and selenium (99.999%) powders. The powders were first mixed in a plastic vial using a mixer before being loaded into a quartz ampoule which was evacuated and sealed. The ampoules were then heated at 1473K for 2 days. In agreement with Hönle et al. [11], x-ray patterns showed that, after this first anneal, the samples contained a significant amount of  $\beta$ -

MoSe<sub>2</sub>. A total of three anneals at 1473K for 2 days each and with intermediate crushing and grinding was necessary to obtain single phase materials. The annealed samples were analyzed by x-ray diffractometry (XRD) after each anneal. The powders were then hot-pressed in graphite dies into dense samples, 10 mm long and 6.35 mm in diameter. The hot-pressing was conducted at a pressure of about 20,000 psi and at temperatures between 1123 and 1273 K for about 2 hours under argon atmosphere.

XRD analysis was performed at room temperature on a Siemens D-500 diffractometer using Cu-K<sub>α</sub> radiation. Small additions of Si powders were made to the samples as an internal standard. Powder X-ray patterns were taken with scan steps of  $2\Theta=0.05^\circ$  and counting time of 3 s. The lattice parameters were calculated from the experimental x-ray patterns using a modified Apple-NBS refinement program [12]. The error in the determination of the lattice parameters was estimated at about  $\pm 0.015$ . Selected samples cut from the hot-pressed bars were polished using standard metallographic techniques. Microprobe analysis (MPA) was performed on these samples to determine their atomic composition using a JEOL JXA-733 electron superprobe operating at  $20 \times 10^3$  Volts (V) of accelerating potential and  $25 \times 10^{-9}$  Amperes (A) of probe current. Pure elements were used as standards and x-ray intensity measurements of peak and background were conducted by wavelength dispersive spectrometry. The density of the samples was calculated from the measured weight and dimensions of the samples.

Samples in the form of disks (typically a 1.0 mm thick, 6.35 mm diameter slice) were cut from the cylinders using a diamond saw (perpendicular to the pressing direction) for electrical and thermal transport property measurements. All samples were characterized at room temperature by Seebeck coefficient, Hall effect and electrical resistivity measurements. High temperature resistivity, Hall effect, Seebeck coefficient, thermal diffusivity, and heat capacity measurements were also conducted on selected samples between room temperature and about 1000K. The electrical resistivity ( $\rho$ ) was measured using the van der Pauw technique with a current of 100 mA using a special high temperature apparatus [13]. The Hall coefficient ( $R_H$ ) was measured in the same apparatus with a constant magnetic field value of  $\sim 10,400$  Gauss. The carrier density was calculated from the Hall coefficient, assuming a scattering factor of 1.0 in a single carrier scheme, by  $p/n = 1/R_H e$ , where  $p$  and  $n$  are the densities of holes and electrons, respectively, and  $e$  is the electron charge. The Hall mobility ( $\mu_H$ ) was calculated from the Hall coefficient and the resistivity values by  $\mu_H = R_H/\rho$ . Errors were estimated to be  $\pm 0.5\%$  and  $\pm 2\%$  for the resistivity and Hall coefficient data, respectively. The Seebeck coefficient ( $\alpha$ ) of the samples was measured on the same samples used for electrical resistivity and Hall coefficient measurements using a high temperature light pulse technique [14]. The error of the Seebeck coefficient measurement was estimated to be less than  $\pm 3\%$ . The heat capacity and thermal diffusivity were measured using a flash diffusivity technique [15]. The thermal conductivity ( $\lambda$ ) was calculated from the

experimental density, heat capacity, and thermal diffusivity values. The overall error in the thermal conductivity measurements was estimated to be about  $\pm 10\%$ .

## Results and discussion

Some properties of two  $\text{Mo}_2\text{Re}_4\text{Se}_8$  are listed in Table I. The density of the samples varies between 94 and 99.7 % of the theoretical value, depending on the pressing temperature. MPA results showed that the samples were slightly different in composition, presumably because of the different temperature used for hot-pressing. Sample DA401 was composed of 95% in volume of a phase with a composition  $\text{Mo}_{13.5}\text{Re}_{29}\text{Se}_{57.5}$  while the remaining 5% phase had a composition  $\text{Mo}_{17.8}\text{Re}_{27.3}\text{Se}_{54.9}$ . For sample DA402, the major phase was  $\text{Mo}_{15.6}\text{Re}_{26.6}\text{Se}_{57.8}$  (about 80% in volume) while the remaining phase had a composition  $\text{Mo}_{13.6}\text{Re}_{28.7}\text{Se}_{57.6}$ . These results show that it is essentially the Mo to Re ratio that changes in the samples indicating that there exists an homogeneity domain centered around the stoichiometric compound  $\text{Mo}_2\text{Re}_4\text{Se}_8$ . Similar results were obtained for the compound  $\text{Mo}_4\text{Ru}_2\text{Se}_8$  [4]. These stoichiometric deviations seem to influence the properties of the samples. Indeed, sample DA401 shows n-type conductivity while sample DA402 is p-type at room temperature (see Table I). The data in Table I suggest that  $\text{Mo}_2\text{Re}_4\text{Se}_8$  is a semiconductor with a low carrier mobility. The high temperature electrical resistivity and Seebeck coefficient values for  $\text{Mo}_2\text{Re}_4\text{Se}_8$  are shown in Figures 2 and 3, respectively. For sample DA401, the electrical resistivity decreases with increasing temperature while the Seebeck coefficient increases, suggesting that both electrons and holes contribute to the conduction. The maximum Seebeck coefficient value for sample DA401 is  $-160 \mu\text{V/K}$  at 1000K. For sample DA402, the electrical resistivity decreases only slightly with increasing temperature while the Seebeck decreases from  $+65 \mu\text{V/K}$  at room temperature to nearly  $0 \mu\text{V/K}$  at 1073K.

The results show that  $\text{Mo}_2\text{Re}_4\text{Se}_8$  is a semiconductor in agreement with previous results [3]. However, significant changes in the transport properties are associated with variations in the Mo to Re ratio the samples. For sample DA401, most of the sample is composed of a phase close to the  $\text{Mo}_2\text{Re}_4\text{Se}_8$  stoichiometry while the dominant phase in sample DA402 is slightly Mo-rich. For sample DA401, n-type conductivity is obtained while p-type conductivity is observed for sample DA402 which possess a more semimetallic behavior. The semiconducting nature of  $\text{Mo}_2\text{Re}_4\text{Se}_8$  is consistent with the theoretical prediction of an energy gap in the band structure of Chevrel phases with a cluster VEC of 4 [6]. Compounds with a cluster VEC lower than 4 are metallic. This is consistent with our results indicating that the Mo-rich sample has a more semimetallic behavior, suggesting a decrease in the energy band gap. The possibility of tailoring the energy gap with composition might be useful when considering the optimization of the thermoelectric properties of Chevrel phases in different temperature ranges and doping levels. Some other semiconducting Chevrel phases are listed in Table II. It is interesting to point out that the compound  $\text{Mo}_4\text{Ru}_2\text{Te}_8$  is metallic although its cluster VEC is 4. It was

found that in  $\text{Mo}_4\text{Ru}_2\text{Se}_{8-x}\text{Te}_x$  compounds, the energy gap is reduced going from the Se-rich materials to Te-rich materials which are semi-metals [4]. A similar result was reported for  $\text{Mo}_2\text{Re}_4\text{X}_8$  materials, i.e. a reduction in energy gap is observed going from the sulfides to the selenides and tellurides.

The thermal conductivity data for  $\text{Mo}_2\text{Re}_4\text{Se}_8$  samples are shown in Figure 4 and the room temperature value is 24 mW/cmK. It decreases steadily with increasing temperature and varies as  $T^{-0.4}$ . This indicates that point defects scattering (resulting from the substitution of Re for Mo) lead a weaker temperature dependence than it would be obtained for acoustic phonons only. The values are relatively low and comparable to state-of-the-art thermoelectric materials. Because mixed conduction occurs in our samples, some of the heat is conducted by both types of carriers and this electronic thermal conductivity accounts to the total thermal conductivity values shown in Figure 4.

The value of a material for thermoelectric applications can be evaluated by a quantity called the thermoelectric figure of merit (ZT) defined as  $ZT = \alpha^2 \rho T / \lambda$ . The larger ZT is, the better the material's conversion efficiency. One of the requirements for a good thermoelectric material is therefore a low thermal conductivity. As it was described by Yvon [1], the stacking of  $\text{Mo}_6\text{X}_8$  units leaves a number of cavities in the lattice which can be filled by a variety of atoms with different sizes. These atoms may be efficient in scattering the phonons as it was established for skutterudite materials [7-10] and first suggested by Slack [17]. The cavities in the Chevrel structure are empty in the binary compounds such as  $\text{Mo}_6\text{Te}_8$  and are filled by the M atoms in the ternary compounds  $\text{M}_x\text{Mo}_6\text{X}_8$ . The largest of the voids in the Chevrel structure has nearly a cubic shape formed by 8 chalcogen atoms as illustrated in Figure 5a. Large atoms such as Pb or La can exclusively occupy these large voids with a filling factor limit corresponding to  $x \sim 1$ . Smaller atoms such as Cu, Ni or Fe, for example can be inserted in 12 different smaller holes with irregular shapes in the chalcogen channels as illustrated in Figure 5b. For small atoms, the upper occupancy limit was experimentally found to be corresponding to  $x=4$ . It is also important to point out that the shapes and sizes of the interstices depend on the composition and degree of filling. The thermal behavior of  $\text{M}_x\text{Mo}_6\text{X}_8$  has been studied by Yvon [1]. One of the results of these studies is that it appears that the M atoms are systematically not confined in a fixed position, are weakly bound and small atoms in particular are able to move between the 12 different lattice sites. The motion of these atoms within the lattice may be particularly efficient in scattering phonons, resulting in low lattice thermal conductivity. The study of  $\text{M}_x\text{Mo}_6\text{X}_8$  ternary compounds would therefore be of great interest.

In  $\text{Mo}_2\text{Re}_4\text{Se}_8$ , most of the scattering of the phonons is produced by mass and volume fluctuations and the thermal conductivity values are already relatively low. If metal atoms can be inserted into the existing voids in the lattice, very low thermal conductivity values could be achieved. However, it was found that only very small amounts of an additional element M such as Sn can be introduced in the compound [3]. This might be explained by

the fact that the cluster VEC is already at 4 and the bands below the gap are completely filled, preventing the insertion additional M elements. Other approaches must thus be considered to study the effect of void fillers on the thermal conductivity of semiconducting Chevrel phases. In the  $\text{Cu}_x\text{Mo}_6\text{S}_8$  system, compositions with  $x=4$  have been reported [16] and, assuming that the Cu has an oxidation state of +1, the ionic formula would be  $\text{Cu}_4^+\text{Mo}_6^{2+}\text{S}_8^{2-}$ . The “magic” cluster VEC number of 4 is met in this compound which should be semiconducting. Another possibility to explore is to prepare semiconducting Chevrel phases combining void fillers and a mixed cluster  $(\text{Mo}_{6-x}\text{M}'_x)$ , where  $\text{M}'$  is a metal) to achieve “magic” VEC number of 4. For example, an hypothetical compound  $\text{Cu}_2\text{Mo}_3\text{Re}_3\text{Se}_8$  would have a cluster VEC of 4 and should be a semiconductor. Such a compound would be particularly attractive because phonons would presumably be scattered by both point defects and the void fillers. The possibilities are obviously numerous but efforts should focus first on determining the impact of the void fillers on the lattice thermal conductivity of semiconducting Chevrel phases. This constitutes the next step in determining the potential of Chevrel phases for thermoelectric applications.

## Conclusion

For the first time, the thermoelectric properties of a semiconducting Chevrel,  $\text{Mo}_2\text{Re}_4\text{Se}_8$ , have been measured. The results confirmed the semiconducting nature of this material predicted by a valence electron count rule per  $[\text{Mo}_6]$  cluster. The thermal conductivity values are relatively low and comparable to those measured for state-of-the-art thermoelectric materials. The crystal structure of the Chevrel phases present cavities which can greatly vary in size and accommodate various atoms ranging from large ones such as Pb to small ones such as Cu. These atoms are not localized in the structure and, depending on their size, can move between different sites. We believe that they can produce a significant phonon scattering and result in low lattice thermal conductivity Chevrel phases. Several compositions were proposed to study the impact of the void fillers on the lattice thermal conductivity of Chevrel phases and continue their assessment for thermoelectric applications.

## Acknowledgments

The work described in this paper was carried out at the Jet Propulsion Laboratory/California Institute of Technology, under contract with the National Aeronautics and Space Administration. We thank A. Borshchevsky and D. Singh for stimulating and valuable discussions. The authors would like to thank Danny Zoltan and Andy Zoltan for thermoelectric property measurements, Paul Carpenter for microprobe analyses, and Jim Kulleck for XRD analyses. This work was supported by the Defense Advanced Research Projects Agency, Grant No. E407.

## References

1. K. Yvon, *Current Topics in Materials Science* (E. Kaldis) Vol. 3, p. 53, North-Holland Amsterdam (1979).
2. R. Chevrel, M. Sergent and J. Pringent, *J. Solid State Chem.* **3**, 515 (1971).
3. A. Perrin, M. Sergent and O. Fischer, *Mat. Res. Bul.* **13**, 259 (1978).
4. A. Perrin, R. Chevrel, M. Sergent and O. Fischer, *J. Solid State Chem.* **33**, 43 (1980).
5. K. Yvon and E. Paoli, *Solid State Communication* **24**, 41 (1977).
6. L. F. Matheiss and C. F. Fong, *Phys. Rev.* **B15**, 1760 (1977).
7. J. -P. Fleurial, A. Borshchevsky, T. Caillat, D. T. Morelli and G. P. Meisner *Proceedings of the XV International Conference on Thermoelectrics*, Pasadena, CA, USA, IEEE Catalog Number 96TH8169, p. 91 (1996).
8. B. C. Sales, D. Mandrus, R. K. Williams, *Science* **272** 1352 (1996).
9. D. T. Morelli and G. P. Meisner, *J. Appl. Phys.* **77** 3777 (1995).
10. G. S. Nolas, G. A. Slack, D. T. Morelli, T. M. Tritt, and A. C. Ehrlich, *J. Appl. Phys.* **79** 4002 (1995).
11. W. Hönlé, H. D. Flack and K. Yvon, *J. Solid State Chem.* **49**, 157 (1983).
12. H. T. Evans, D. E. Appleman and D. S. Handwerker, *Report # PB216188*, U.S. Dept. of Commerce, National Technical Information Center, 5285 Port royal Road Springfield, VA 22151 (1973).
13. J. A. McCormack and J. -P. Fleurial, *Modern Perspectives on Thermoelectrics and Related Materials*, MRS Symp. Proc. **234** (Materials Research Society, Pittsburgh, Pennsylvania ), p. 135 (1991)
14. C. Wood C., D. Zoltan and G. Stapfer, *Rev. Sci. Instrum.* **56**, 5, 719 (1985).
15. J. W. Vandersande, C. Wood, A. Zoltan and D. Whittenberger, *Thermal Conductivity* , Plenum Press, New York, 445 (1988).
16. D. C. Johnston, R. N. Shelton, and J. J. Bugaj, *Solid State Communication* **21**, 949 (1977).
17. G. A. Slack, *Thermoelectric Handbook*, edited by M. Rowe (CRC, Boca Raton, FL, 1995), p. 407.

## Tables caption

Table I. Properties of  $\text{Mo}_2\text{Re}_4\text{Se}_8$  samples at room temperature.

Table II. List of semiconducting Chevrel phases.

## Figures captions

Figure 1. Illustration of the  $\text{Mo}_6\text{X}_8$  ( $\text{X}=\text{S}, \text{Se}, \text{Te}$ ) building block of the rhombohedral Chevrel phase structure.

Figure 2. Electrical resistivity versus inverse temperature for two polycrystalline  $\text{Mo}_2\text{Re}_4\text{Se}_8$  samples (see text for the exact composition of the samples).

Figure 3. Seebeck coefficient versus temperature for two polycrystalline  $\text{Mo}_2\text{Re}_4\text{Se}_8$  samples (see text for the exact composition of the samples).

Figure 4. Thermal conductivity versus temperature for two polycrystalline  $\text{Mo}_2\text{Re}_4\text{Se}_8$  sample (see text for the exact composition of the samples and Table I for density values). Values for state-of-art thermoelectric materials are also presented for comparison:  $\text{Bi}_2\text{Te}_3$  and  $\text{PbTe}$  based alloys and TAGS (Te-Ag-Ge-Se alloys).

Figure 5. Illustrations showing the positions of filling atoms in the cavities of the Chevrel crystal structure (after reference 1). The figures represent a projection of the crystal structure on the hexagonal  $(11\bar{2}0)$  plane. The large atoms of Pb in  $\text{PbMo}_6\text{S}_8$  occupy a cube shaped chalcogen hole (5a) whereas small Cu atoms can be distributed over 12 different sites in the chalcogen network of  $\text{Cu}_x\text{Mo}_6\text{S}_8$  ( $x_{\text{max}}=4$ ) (5b).



		Sample	DA401	DA402
Property	Units			
$a_H$	Å		9.667	9.667
$c_H$	Å		10.738	10.738
Hot-pressing temperature	K		1123	1273
X-ray density	$\text{g/cm}^3$		8.97	8.97
Experimental density	$\text{g/cm}^3$		8.41	8.95
Electrical resistivity	$\text{m}\Omega\cdot\text{cm}$		72	14
Hall mobility	$\text{cm}^2/\text{V s}$		0.09	0.23
Hall carrier concentration	$10^{21}/\text{cm}^3$		0.91	1.97
Seebeck coefficient	$\mu\text{V/K}$		-70	65
Thermal conductivity	$\text{mW/cm K}$		24	-

Table I

Material	Cluster VEC	Type of conductivity	Reference
$\text{Mo}_2\text{Re}_4\text{S}_8$	4	semiconductor	3
$\text{Mo}_2\text{Re}_4\text{Se}_8$	4	semiconductor	3
$\text{Mo}_4\text{Ru}_2\text{Se}_8$	4	semiconductor	4
$\text{Mo}_2\text{Re}_4\text{S}_{8-x}\text{Se}_x$ ( $0 \leq x \leq 8$ )	4	semiconductor	3
$\text{Mo}_2\text{Re}_4\text{Se}_{8-x}\text{Te}_x$ ( $0 \leq x \leq 1.2$ )	4	semiconductor	3
$\text{Mo}_4\text{Ru}_2\text{Se}_{8-x}\text{Te}_x$ ( $0 \leq x \leq 1$ )	4	semiconductor	4
$\text{Mo}_4\text{Ru}_2\text{Te}_8$	4	metallic	4

Table II

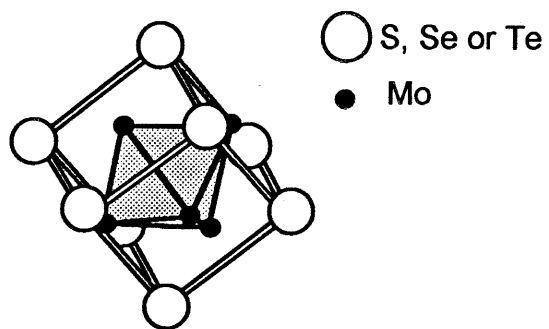


Figure 1

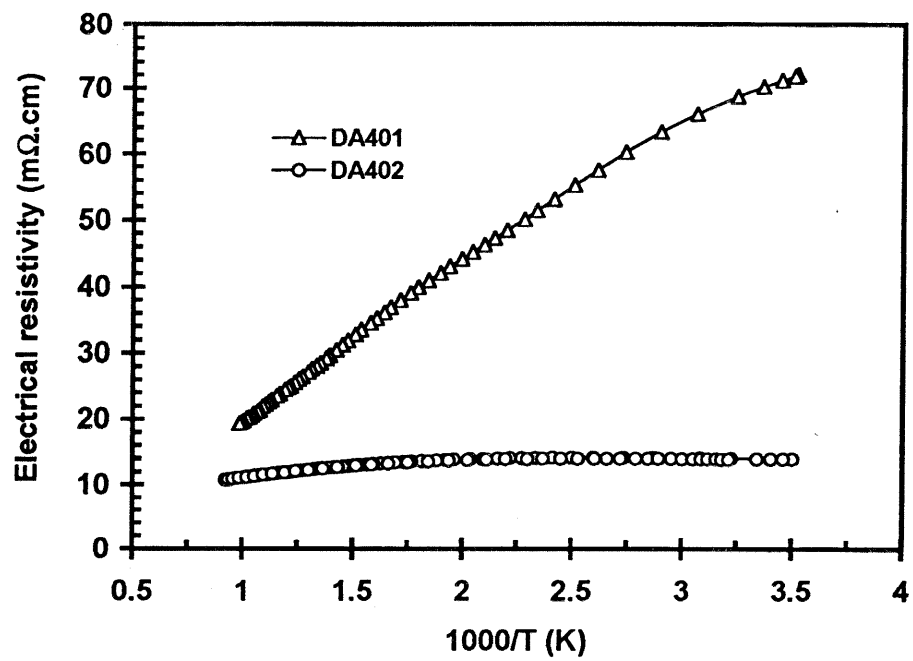


Figure 2

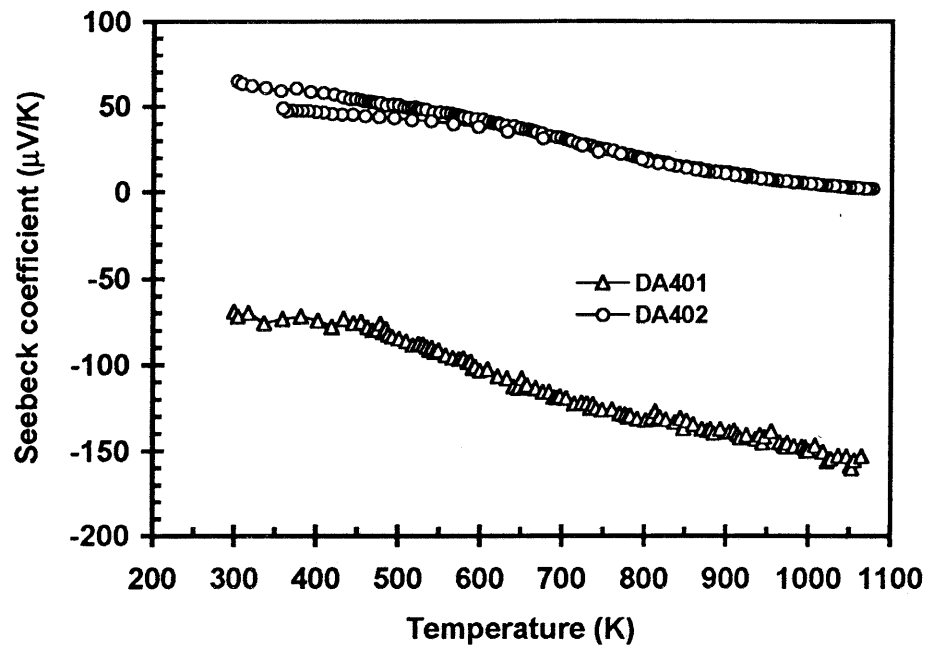


Figure 3

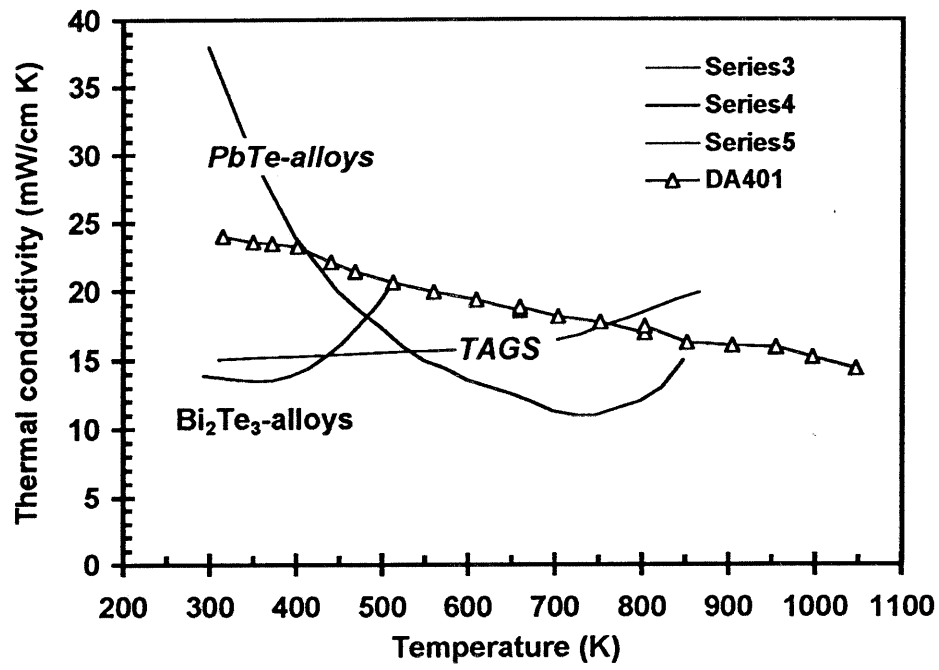
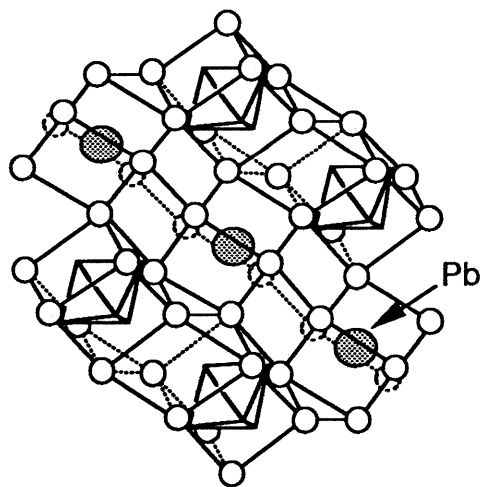
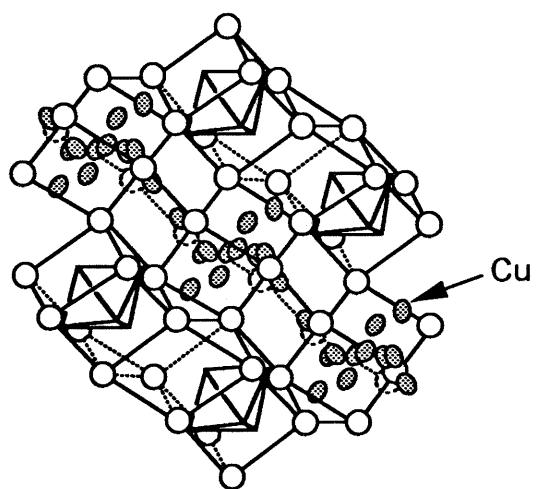


Figure 4



(a)  $\text{PbMo}_6\text{S}_8$



(b)  $\text{Cu}_x\text{Mo}_6\text{S}_8$